

DPNU-98-08
UT-805Numerical Study of the Double Scaling Limit
in Two-Dimensional Large N Reduced ModelTakayuki NAKAJIMA¹⁾ * AND Jun NISHIMURA²⁾ †

- 1) *Department of Physics, University of Tokyo,
Bunkyo-ku, Tokyo 113, Japan*
- 2) *Department of Physics, Nagoya University,
Chikusa-ku, Nagoya 464-01, Japan*

Abstract

We study the two-dimensional Eguchi-Kawai model as a toy model of the IIB matrix model, which has been recently proposed as a nonperturbative definition of the type IIB superstring theory. While the planar limit of the model is known to reproduce the two-dimensional Yang-Mills theory, we find through Monte Carlo simulation that the model allows a different large N limit, which can be considered as the double scaling limit in matrix models.

*E-mail address : nakajima@danjuro.phys.s.u-tokyo.ac.jp
†E-mail address : nisimura@eken.phys.nagoya-u.ac.jp

1 Introduction

It is no doubt that the nonperturbative study of string theories is one of the most exciting topic in particle physics, since it might provide all the answers to the fundamental questions concerning our world, such as the space-time dimension, the gauge group, the three generations of the matter fields and so on. Indeed the nonperturbative study of the bosonic string theory in less than one dimension was successfully done through the double scaling limit of the matrix model [1] some time ago. Much effort has been made towards the generalization of the approach to bosonic strings in more than one dimensions [2, 3] as well as to superstrings [4, 5].

Recently, a new type of matrix model has been proposed as a nonperturbative definition of the superstring theory. The model proposed by Banks, Fischler, Shenker and Susskind [6], which is conjectured to provide a nonperturbative definition of the M-theory [7] in the infinite-momentum frame, is a matrix quantum mechanics, which can be obtained by dimensional reduction of the 10D large N super Yang-Mills theory to one dimension, while the one proposed by Ishibashi, Kawai, Kitazawa and Tsuchiya [8], which is conjectured to provide a nonperturbative definition of type IIB superstring theory, is a matrix model, which can be obtained by dimensional reduction of the 10D large N super Yang-Mills theory to a point. It is now conventional to call the former as M(-atrix) theory and the latter as IIB matrix model. Although these proposals are basically based on the spirit to describe the strings in terms of matrices of very large size, there are many novel features that didn't show up in the old-fashioned matrix models. One of them is the appearance of the Yang-Mills theory. This is related to the effective action [9] of D-particles and D-instantons, respectively for the two models. It can also be viewed to be related to the supermembrane action and the Green-Schwartz action in the Schild gauge, respectively. Another interesting feature of these models is that all the target-space coordinates come out as the eigenvalues of the matrices.

For the IIB matrix model, the light-cone string field Hamiltonian of the type IIB superstring theory has been reproduced [10] by identifying the string field for fundamental strings with the Wilson loop and analyzing the Schwinger-Dyson equation. As an important consequence of this study, they have clarified how one should take the double scaling limit in this model. The IIB matrix model can be considered as an example of large N reduced models (See Ref. [11] for a review.), which have been studied so far exclusively in the planar limit, in which the models are equivalent to the field theory before being reduced. Whether a large

N reduced model allows any sensible double scaling limit is itself a nontrivial question.

In this paper, we study the two-dimensional Eguchi-Kawai model [12], as a toy model of the IIB matrix model. The model is nothing but the $SU(N)$ lattice gauge theory on a 1×1 lattice with the periodic boundary condition and it is equivalent to the $SU(N)$ lattice gauge theory on the infinite lattice in the planar limit. We perform a Monte Carlo simulation of the model and find that the model indeed allows a different large N limit, which can be considered as the double scaling limit in matrix models.

The paper is organized as follows. In section 2, we give the definition of the model and review some known results. We also explain the algorithm we use in our simulation. In section 3, we study the planar limit of the model. We show how the finite N effects appear by measuring Wilson loops. This gives us an important clue to a possible double scaling limit. In section 4, we present the data which show the existence of the double scaling limit in the model. Section 5 is devoted to conclusions and discussions.

2 The model

The Eguchi-Kawai (EK) model is defined by the following action [12].

$$S_{EK} = -N\beta \sum_{\mu \neq \nu=1}^D \text{tr}\{U_\mu U_\nu U_\mu^\dagger U_\nu^\dagger\}, \quad (2.1)$$

This model has the $U(1)^D$ symmetry.

$$U_\mu \rightarrow e^{i\theta_\mu} U_\mu. \quad (2.2)$$

In Ref. [12], it has been shown that if the $U(1)^D$ symmetry is not spontaneously broken, the model is equivalent to the $SU(N)$ lattice gauge theory on the infinite lattice in the large N limit, where the coupling constant β in the action (2.1) is kept fixed. This limit is referred to as the planar limit, since in this limit Feynman diagrams with planar topology dominate.

By equivalence, we mean that the expectation value of the Wilson loop

$$W(C) = \frac{1}{N} \text{tr} \left\{ U_{x,\alpha} U_{x+\hat{\alpha},\beta} U_{x+\hat{\alpha}+\hat{\beta},\gamma} \cdots U_{x-\hat{\lambda},\lambda} \right\}, \quad (2.3)$$

which is the product of link variables along a closed loop C , calculated within the lattice gauge theory with the action

$$S_{LGT} = -N\beta \sum_x \sum_{\mu \neq \nu=1}^D \text{tr}\{U_{x,\mu} U_{x+\hat{\mu},\nu} U_{x+\hat{\nu},\mu}^\dagger U_{x,\nu}^\dagger\}, \quad (2.4)$$

is equal to the expectation value of the corresponding observable

$$w(C) = \frac{1}{N} \text{tr} \{ U_\alpha U_\beta U_\gamma \cdots U_\lambda \}, \quad (2.5)$$

calculated within the EK model with the action (2.1) in the planar limit.

It is found in Ref. [13] that when the space-time dimension D is larger than two, the $U(1)^D$ symmetry is spontaneously broken in the weak coupling region $\beta \gg 1$. This means that we cannot study the continuum limit of the large N gauge theory by the EK model when $D > 2$, since we have to send β to infinity when we take the continuum limit. However, it is found that when D is even, one can twist the boundary condition of the EK model so that the $U(1)^D$ symmetry is not broken in the weak coupling region, while keeping the proof of the equivalence valid. This is the twisted Eguchi-Kawai (TEK) model [14] defined by the action

$$S_{TEK} = -N\beta \sum_{\mu \neq \nu=1}^D Z_{\mu\nu} \text{tr} \{ U_\mu U_\nu U_\mu^\dagger U_\nu^\dagger \}, \quad (2.6)$$

where $Z_{\mu\nu}$ is called as the ‘twist’, and defined as

$$Z_{\mu\nu} = Z_{\nu\mu}^* = \exp(2\pi i/L) \quad \text{for } \mu < \nu, \quad (2.7)$$

where $N = L^{D/2}$. The observable that corresponds to the Wilson loop $W(C)$ is now given by

$$w(C) = \frac{1}{N} \left(\prod_{\mu < \nu} Z_{\mu\nu}^{P_{\mu\nu}} \right) \text{tr} \{ U_\alpha U_\beta U_\gamma \cdots U_\lambda \}, \quad (2.8)$$

where $P_{\mu\nu}$ is the number of plaquettes in the $(\mu\nu)$ direction on the surface spanned by the Wilson loop C . The TEK model has been recently used for searching for nontrivial fixed points in the six-dimensional large N gauge theory [15].

In two dimensions, since the $U(1)^2$ symmetry is not spontaneously broken even in the weak coupling region, the EK model is equivalent to the lattice gauge theory in the planar limit in the above sense. The two-dimensional lattice gauge theory is solvable [16] in the planar limit and indeed the exact results obtained there has been reproduced by the EK model in the planar limit [12]. On the other hand, the TEK model can be considered in two dimensions as well, and its planar limit should be the same as that of the EK model. Note, however, that the two models can show different finite N effects, which is relevant to us, since we are aiming at discovering a large N limit other than the planar limit. Indeed we see that the approach to the planar limit from finite N is quite different for the two models, and the double scaling limit seems to exist only for the EK model.

Let us explain the algorithm we use for the Monte Carlo simulation of the EK and TEK models. Since the actions of the two models (2.1) and (2.6) are not linear in terms of link variables unlike that of the ordinary lattice gauge theory (2.4), we cannot apply the heat bath method [17] as it stands. We therefore employ the technique proposed by Ref. [18], and introduce the auxiliary field $Q_{\mu\nu}$ ($\mu < \nu$), which are general complex $N \times N$ matrices, with the following action.

$$\begin{aligned} S = & N\beta \sum_{\mu < \nu} \text{tr} Q_{\mu\nu}^\dagger Q_{\mu\nu} \\ & - N\beta \sum_{\mu < \nu} \text{tr} Q_{\mu\nu}^\dagger (t_{\mu\nu} U_\mu U_\nu + t_{\nu\mu} U_\nu U_\mu) \\ & - N\beta \sum_{\mu < \nu} \text{tr} Q_{\mu\nu} \left(t_{\mu\nu}^* U_\mu^\dagger U_\nu^\dagger + t_{\nu\mu}^* U_\nu^\dagger U_\mu^\dagger \right), \end{aligned} \quad (2.9)$$

where $t_{\mu\nu}$ is 1 for the EK model and is $\sqrt{Z_{\mu\nu}}$ for the TEK model. Integrating out the auxiliary field $Q_{\mu\nu}$, one reproduces the original actions of the reduced models. The update of $Q_{\mu\nu}$ can be done easily by generating Gaussian variables. Note that the action (2.9) is linear in terms of U_μ , which means that we can apply the heat bath method. The update of U_μ is carried out by successively multiplying it by matrices each belonging to the $N(N-1)/2$ SU(2) subgroups of SU(N) [19]. We define ‘one sweep’ in this paper by the update of all the elements of $Q_{\mu\nu}$ ’s and the update of all the U_μ ’s by multiplying elements of every SU(2) subgroup once for each.

3 Planar limit and the finite N effects

In this section, we see how the EK model and the TEK model at finite N approach the known results in the planar limit as one increases N with fixed β in the action (2.1) and (2.6), respectively.

The observables calculated by Gross-Witten [16] for the two-dimensional SU(N) lattice gauge theory in the planar limit is the Wilson loop $W(C)$, where the contour C is a rectangle. Due to the discrete translational and rotational invariance and the parity invariance of the lattice gauge theory, the expectation value of Wilson loops is real and it depends only on its shape but not on how the loop is placed on the lattice nor on the orientation of the loop. We therefore denote the expectation value of the $I \times J$ Wilson loop by $\langle W(I \times J) \rangle$.

We examine what we get for the corresponding observables (2.5) and (2.8) in the reduced models with finite N . Just as we mentioned above for the lattice gauge theory, the

expectation value of the observable in the EK model that corresponds the Wilson loop is real and it depends only on its shape even for finite N due to the symmetries : $U_1 \rightarrow U_2$ and $U_2 \rightarrow U_1^\dagger$, which corresponds to the rotational symmetry, and $U_1 \rightarrow U_2$ and $U_2 \rightarrow U_1$, which corresponds to the parity invariance. This is not the case, however, with the TEK model, in which the second one ('parity transformation') is not a symmetry. Accordingly, the expectation value of the observable in the finite N TEK model that corresponds to the Wilson loop is not real and it becomes complex conjugate when one flips the orientation of the loop, though the imaginary part should vanish in the planar limit, where it should reproduce the Wilson loop in the lattice gauge theory. When we define $\langle w(C) \rangle$ in reduced models which corresponds to $\langle W(C) \rangle$ in the lattice gauge theory, the real part is implicitly taken in the case of the TEK model. When we measure $\langle w(C) \rangle$ in either model, we average over the transformation of the Wilson loop by rotation and parity in order to increase the statistics.

The internal energy of the system can be given by the expectation value of the 1×1 Wilson loop

$$E(\beta) = \langle W(1 \times 1) \rangle, \quad (3.1)$$

and the analytical result in the planar limit is obtained as [16]

$$E(\beta) = \begin{cases} \beta & \text{for } \beta \leq \frac{1}{2} \\ 1 - \frac{1}{4\beta} & \text{for } \beta \geq \frac{1}{2}. \end{cases} \quad (3.2)$$

As one sees from this result, the second derivative of the internal energy is discontinuous at $\beta = 1/2$, which means that the system undergoes a third-order phase transition at $\beta = 1/2$.

In Fig. 1, we plot the internal energy against β for the two models for $N = 32$. We can see that the data agree nicely to the theoretical result in the planar limit (3.2), which is represented by the solid line. In Ref. [14], the results for $N = 20$ are given, which shows that the data for the EK model are slightly larger than the planar result, while the data for the TEK model are in complete agreement with it. This tendency has been observed in our simulation as well with smaller N . Thus as far as the internal energy is concerned, the convergence to the planar limit is better for the TEK model than for the EK model.

Let us turn to the expectation value of rectangular Wilson loops of various size. The planar result is given by

$$\langle W(I \times J) \rangle = \exp(-\kappa(\beta)IJ), \quad (3.3)$$

internal energy in EK/TEK model

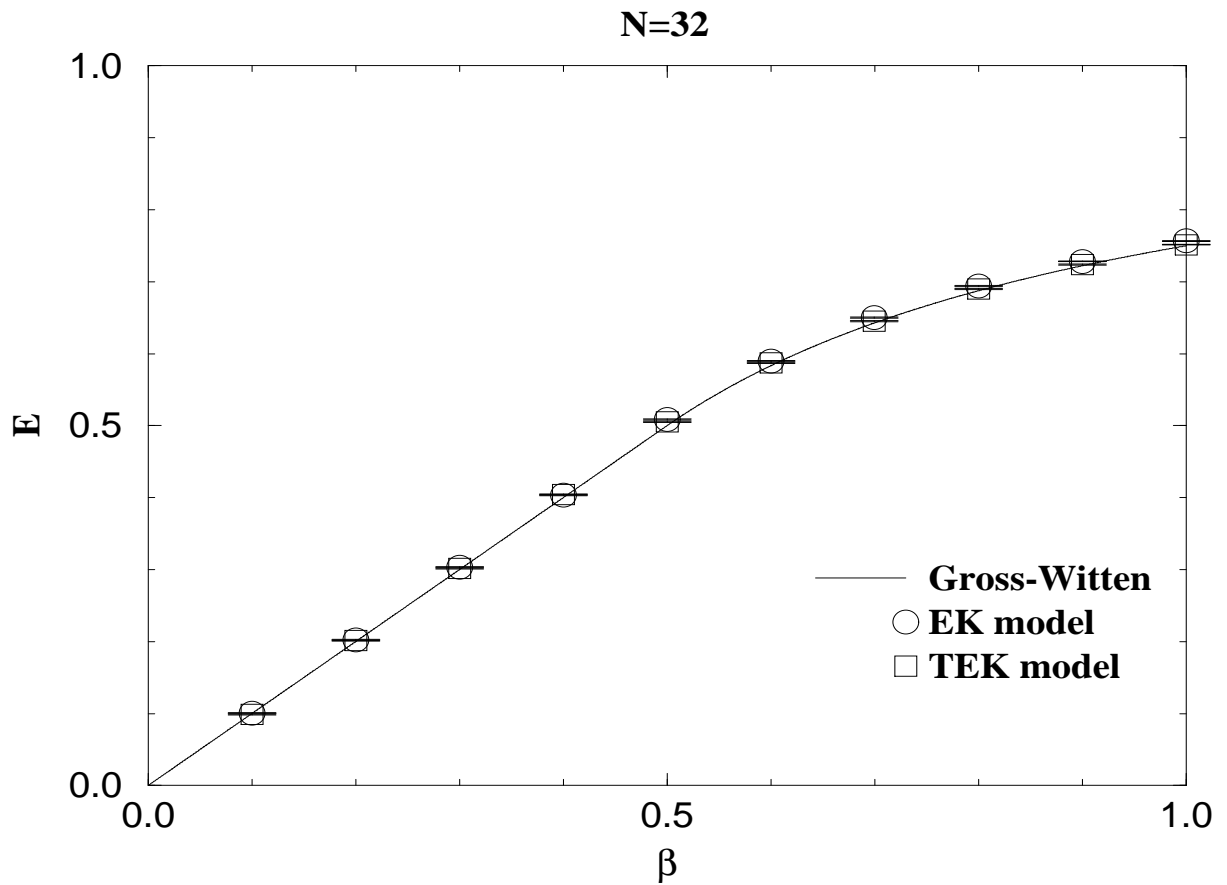


Figure 1: The internal energy is plotted against β for the EK model (circles) and for the TEK model (squares) for $N = 32$. The solid line represents the theoretical result in the planar limit ($N \rightarrow \infty$ with fixed β) obtained by Gross-Witten.

rectangular Wilson loop of various size

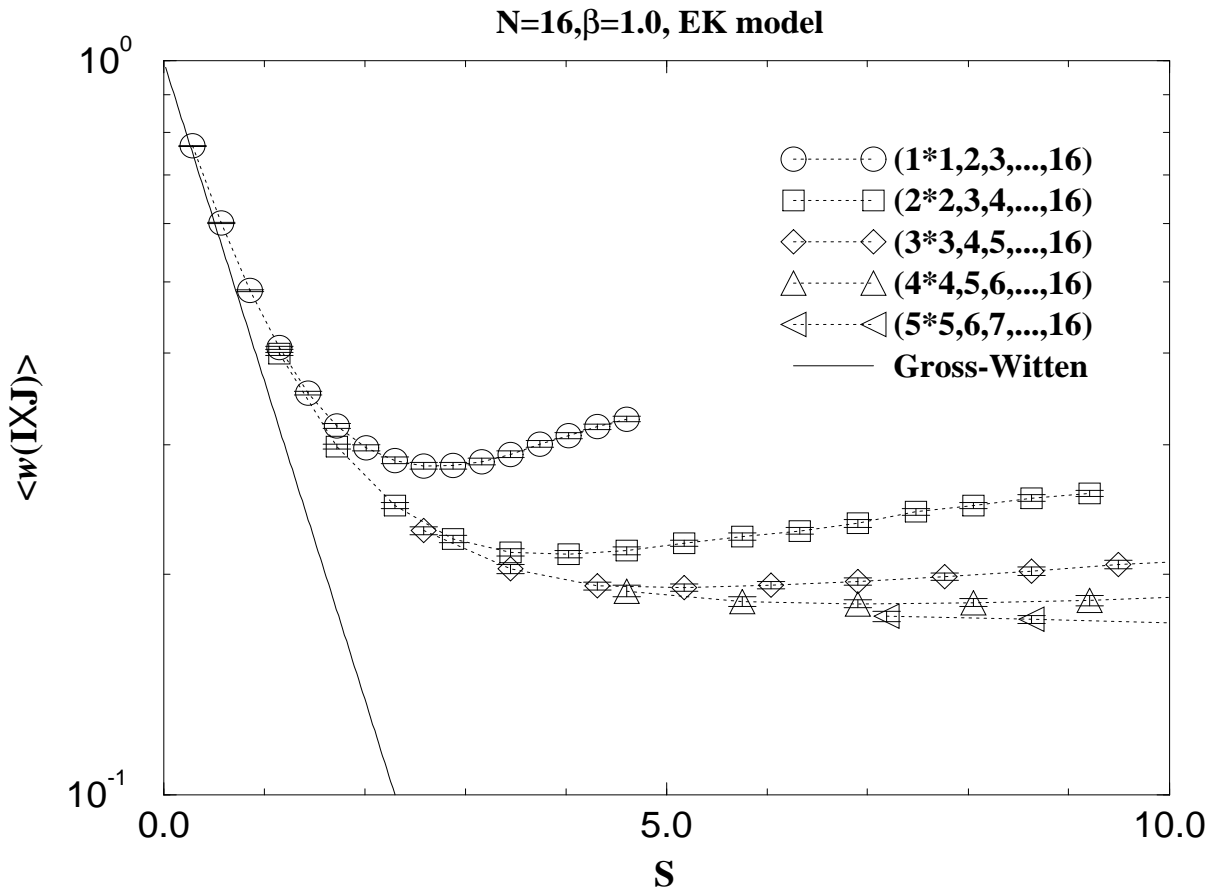


Figure 2: The expectation value of $w(I \times J)$ in the EK model ($N = 16$, $\beta = 1.0$) which corresponds to $I \times J$ Wilson loops is plotted against the physical area $S = a^2 IJ$. Each symbol represents the data for $I = 1$ (circles), $I = 2$ (squares), $I = 3$ (diamonds), $I = 4$ (triangles) and $I = 5$ (tilted triangles) with $J \geq I$. The straight solid line represents the planar result by Gross-Witten.

where

$$\kappa(\beta) = \begin{cases} -\log \beta & \text{for } \beta \leq \frac{1}{2} \\ -\log \left(1 - \frac{1}{4\beta}\right) & \text{for } \beta \geq \frac{1}{2} \end{cases} \quad (3.4)$$

For $I = J = 1$, the above result reduces to the one for the internal energy (3.2). This result shows that the rectangular Wilson loops obey the area law exactly for all β . From this result, one can figure out how to fine-tune the coupling constant β as a function of the lattice spacing a when one takes the continuum limit $a \rightarrow 0$. Since the physical area is given by $S = a^2 IJ$, we have to fine-tune β so that $\kappa(\beta)/a^2$ is kept fixed. We therefore take

$$a = \sqrt{\kappa(\beta)} \quad (3.5)$$

in the following. Since $\kappa(\beta)$ is given by eq. (3.4), we have to send β to infinity as we take the $a \rightarrow 0$ limit.

In Fig. 2, we plot the expectation value of $I \times J$ Wilson loops in the EK model against the physical area $S = a^2 IJ$ for $N = 16$ and $\beta = 1.0$, where I and J run from 1 to 16. Although the planar result depends only on the area of the Wilson loop, but not on its shape, we see that the results for finite N depend on the shape as well. For example, we see that the result for the 1×9 Wilson loop is farther from the planar limit than that for the 3×3 Wilson loop. In general, one sees that the finite N effect for Wilson loops with the same area becomes larger as it becomes longer in one direction. This means that we have to specify not only the area but also the shape of the Wilson loop when we discuss the scaling behavior in the double scaling limit, as well as when we discuss the finite N effects.

In Fig. 3 we plot the expectation value of square Wilson loops in the EK model against the physical area $S = (aI)^2$ for $\beta = 4.0$ with $N = 16, 32, 64$ and 128 . One can see that the data points approach the planar result from above monotonously. In Fig. 4 we plot the deviation of the data for fixed Wilson loops from the planar result as a function of N for $\beta = 1.0$. One can see a clear $1/N^2$ behavior, which means that the deviation is dominated by the subleading term in the large N limit. For $\beta = 4.0$, the deviation decreases slower than $1/N^2$ up to $N = 128$, which means that the contribution from the higher order terms is still comparable with the subleading term. The double scaling limit we consider in the next section corresponds to taking the large N limit together with the $\beta \rightarrow \infty$ limit so that all the terms in the $1/N^2$ expansion contribute.

The finite N effects for the TEK model appear in quite a different manner. Fig. 5 shows the results for the TEK model for the same set of values of N and with the same β as in Fig. 3. One sees from the results for fixed area with $S < 2.5$ that the data do not approach the

square Wilson loop in EK model

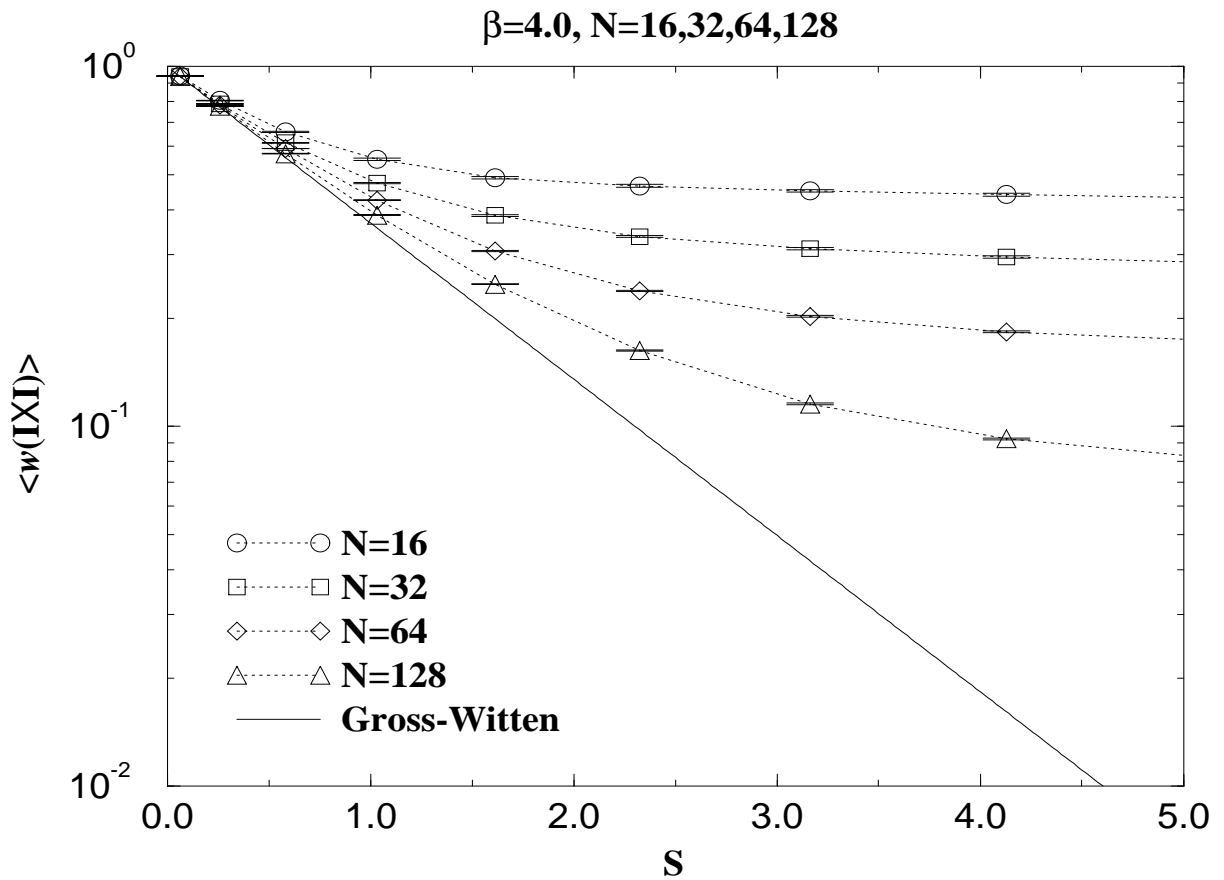


Figure 3: The expectation value of $w(I \times I)$ in the EK model for $\beta = 4.0$ is plotted against the physical area $S = (aI)^2$. Each symbol represents the data for $N = 16$ (circles), $N = 32$ (squares), $N = 64$ (diamonds) and $N = 128$ (triangles). The straight solid line represents the planar result by Gross-Witten.

convergence in large N

$\beta=1.0, \text{EK model}$

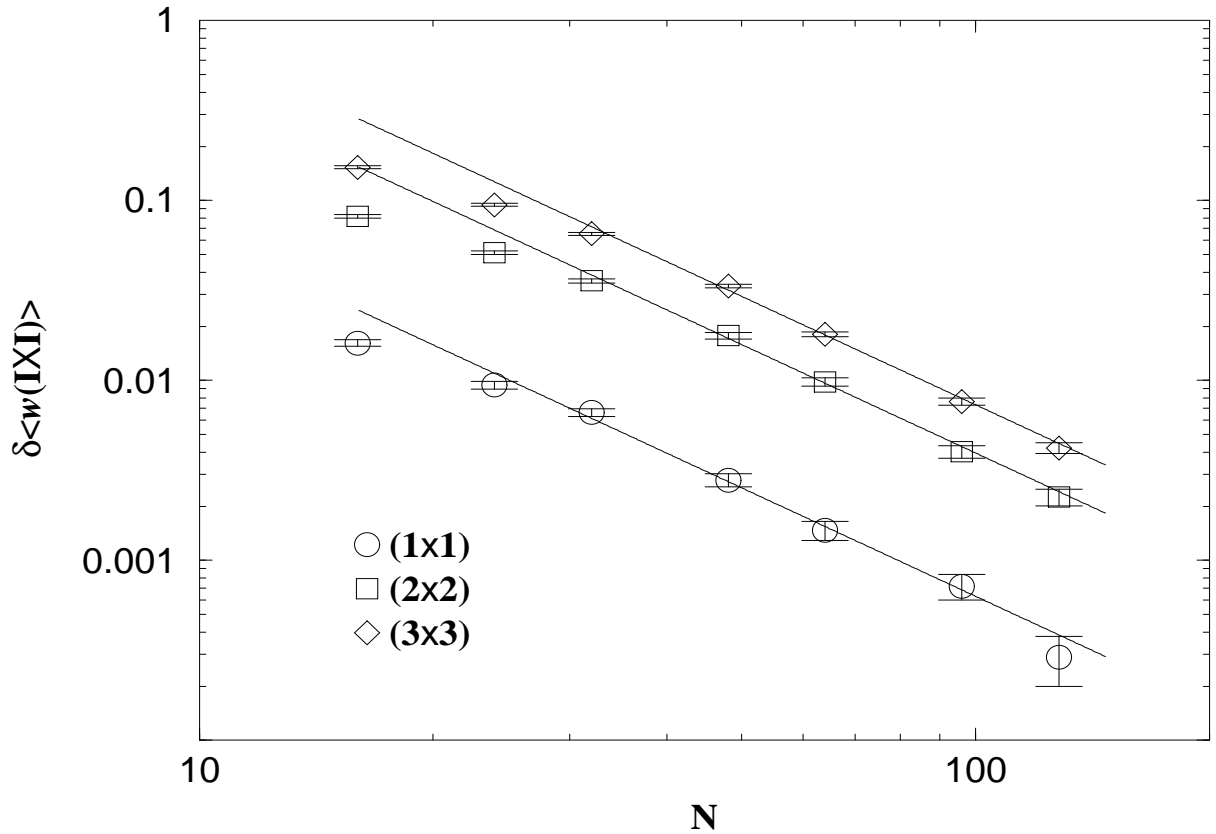


Figure 4: The deviation of the expectation value of $w(I \times I)$ in the EK model from the planar result is plotted against N for $I = 1$ (circles), $I = 2$ (squares) and $I = 3$ (diamonds) at $\beta = 1.0$. The solid straight line represents a fit to $\text{const.}/N^2$, which is the dominant subleading term in the large N limit.

planar result monotonously, but rather show some overshooting behavior. For larger S , the tendency of convergence is not yet seen up to $N = 128$. Thus, although it might be that the convergence to the planar limit is somewhat accelerated in the TEK model as is seen from the results for smaller Wilson loops, we find that the finite N effects in the TEK model are much more complicated than in the EK model.

Another interesting quantity known in the planar limit is the expectation value of Wilson loops with self-intersections [20]. In Fig. 6, we illustrate a typical Wilson loop we consider. It is given by the trace of the product of link variables along the loop $C = abcdaefghia$. We split the original loop C into two loops at the self-intersection point and define $C_1 = abcd$ and $C_2 = aefghia$.

The expectation value of such a Wilson loop has been calculated [20] by solving the Makeenko-Migdal equation [21] in the continuum and the result is given by

$$\langle W(C) \rangle = (1 - 2KS(C_1)) \exp [-K\{S(C_1) + S(C_2)\}]. \quad (3.6)$$

$S(C)$ is the physical area of the region surrounded by the loop C . When $S(C_1) = 0$, the above expression reduces to the one for the Wilson loop without self-interactions, which obeys the area law. K is the physical string tension, which is taken to be 1 in this paper, since we have fixed the scale by eq. (3.5). When $S(C_1) > 0$, the factor $(1 - 2KS(C_1))$ gives a nontrivial correction. We measure the observable

$$w(C) = \frac{1}{N} \text{tr} \left(U_1^L U_2^{L_1} U_1^{\dagger L} U_2^{\dagger L_1} U_1^L U_2^{L_2} U_1^{\dagger L} U_2^{\dagger L_2} \right), \quad L_1 \leq L_2, \quad (3.7)$$

in the EK model and the corresponding one in the TEK model, where we multiply the above expression by $Z_{12}^{L(L_1+L_2)}$ according to the definition (2.8). Comparison with the continuum result in the planar limit (3.6) can be made by putting $S(C_1) = a^2 LL_1$ and $S(C_2) = a^2 LL_2$. In order to extract the nontrivial factor $(1 - 2KS(C_1))$, where $K = 1$, we measure the expectation value $\langle w(C) \rangle$ with fixed $S(C_1) + S(C_2)$ and plot the result against $S(C_1)$. Specifically, we take $L = 1$ and consider L_1 and L_2 with $L_1 + L_2 = 8$ and $L_1 = 0, 1, 2, 3, 4$. The observable for $L_1 = 0$ is nothing but the $(L \times L_2)$ Wilson loop. Fig. 7 and Fig. 8 shows the results for $N = 32$ and $N = 64$ respectively. The planar results by Kazakov-Kostov are shown by the straight heavy solid lines. One sees that the data are on the lines parallel to the planar results, and the lines are slightly above the planar results for the EK model, and slightly below the planar results for the TEK model¹. The discrepancy is smaller for $N = 64$ than for $N = 32$.

square Wilson loop in TEK model

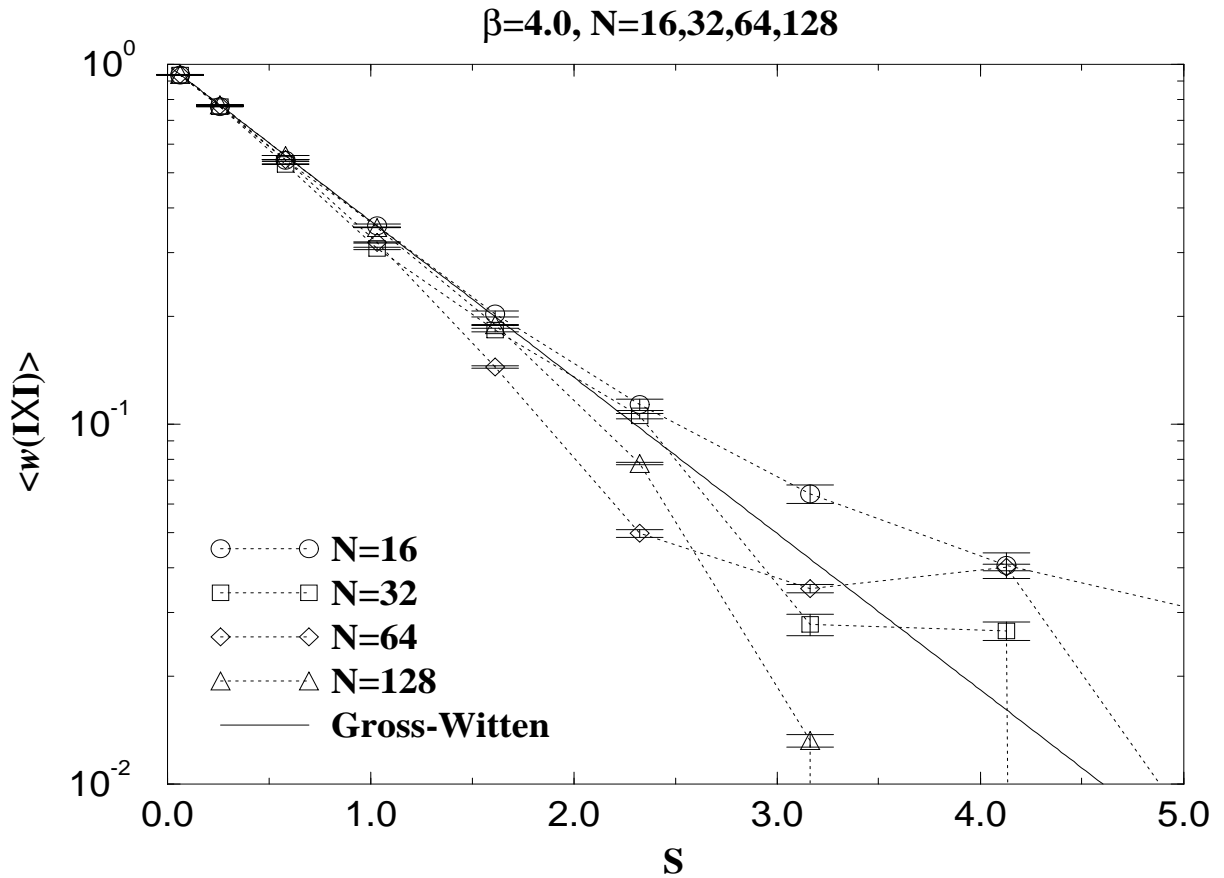


Figure 5: The expectation value of $w(I \times I)$ in the TEK model for $\beta = 4.0$ is plotted against the physical area $S = (aI)^2$. Each symbol represents the data for $N = 16$ (circles), $N = 32$ (squares), $N = 64$ (diamonds) and $N = 128$ (triangles). The straight solid line represents the planar result by Gross-Witten.

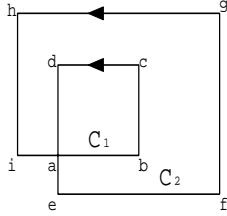


Figure 6: A typical Wilson loop with a self-interaction

This shows that the finite N effect comes mainly from the area law part, and the correction due to the factor $(1 - 2KS(C_1))$ in (3.6) does not show any significant finite N effect. We also note that the total physical area $S(C_1) + S(C_2)$ is 0.516 for $\beta = 4.0$ and the tendency of convergence to the planar limit is consistent with that observed in Fig. 3 and Fig. 5.

4 Existence of double scaling limit in EK model

In this section, we consider the EK model not as a reduced model which reproduce the lattice gauge theory in the planar limit, but as a matrix model which defines a string theory. We therefore examine whether we can take a large N limit other than the planar limit discussed in the previous section.

We consider the EK model as a toy model of the IIB matrix model. Just as in Ref. [8, 10], we make the T-duality transformation, when we interpret the EK model as a string theory. Upon the T-duality transformation, the compactification radius of the torus to which the space time is compactified is inversed and the winding mode and the momentum mode are exchanged. Since the EK model can be considered to be defined on a unit cell of size a with the periodic boundary condition, it can be considered, after the T-duality transformation, as a string theory in the two-dimensional space time compactified on a torus of size $1/a$.

The observables we consider in this section is the Wilson loops

$$\text{tr} \{ U_\alpha U_\beta U_\gamma \cdots U_\lambda \}, \quad (4.1)$$

where the suffix $\alpha, \beta, \dots, \lambda$ runs over $\pm 1, \pm 2$ and $U_{-\alpha}$ ($\alpha > 0$) is defined by $U_{-\alpha} = U_\alpha^\dagger$. The winding number of the Wilson loop is given by $n_\mu = \hat{\alpha}_\mu + \hat{\beta}_\mu + \cdots + \hat{\lambda}_\mu$, where $\hat{\alpha}_\mu$ denotes

¹Strictly speaking, L , L_1 and L_2 should be large enough when we compare the data with the continuum result. The data show, however, that the finite lattice spacing effect is absent accidentally for the observable considered, as in the case with the simple rectangular Wilson loops, which obey the area law exactly even for the (1×1) loop.

Wilson loop with self-intersection

N=32

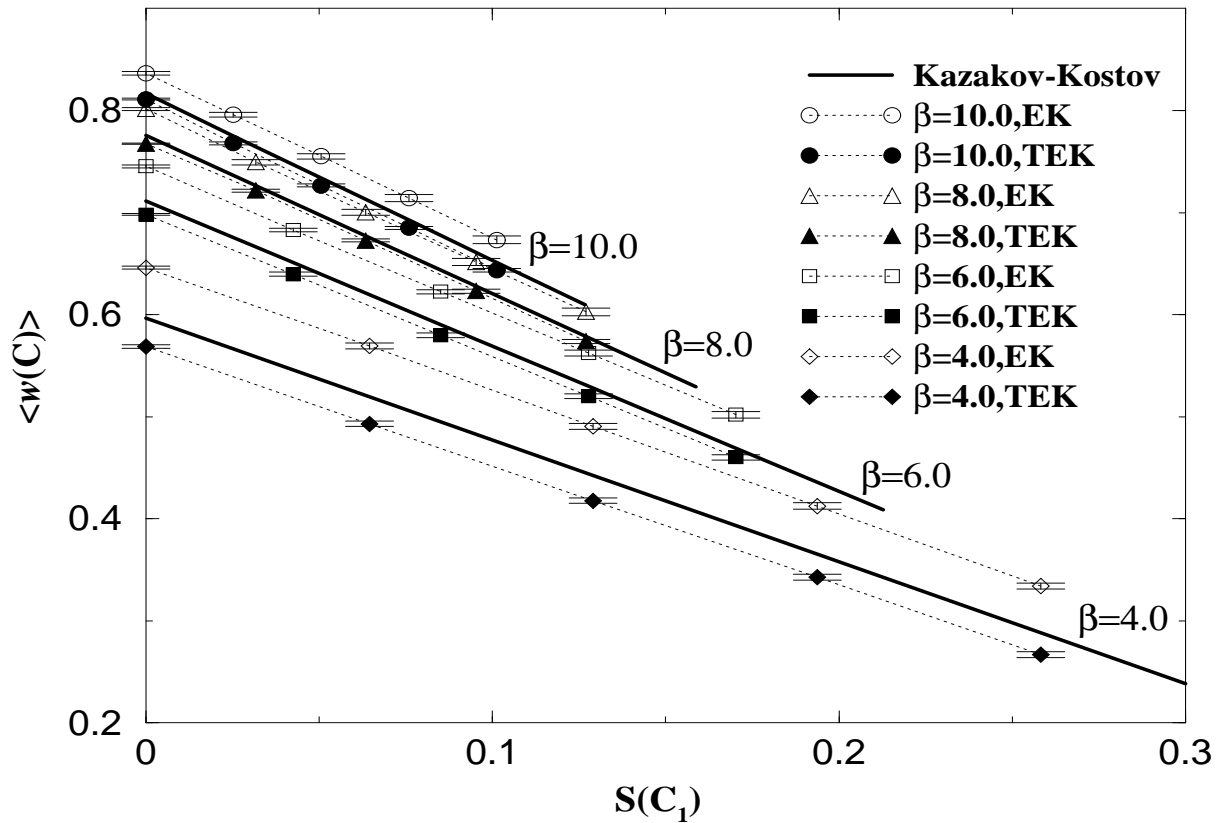


Figure 7: The expectation value of $w(C)$ in the EK (open symbols) and the TEK model (filled symbols) for $N = 32$ with $\beta = 4.0$ (diamonds), 6.0 (squares), 8.0 (triangles) and 10.0 (circles) are plotted against the physical area $S(C_1) = a^2 LL_1$. The straight heavy solid lines represent the continuum results in the planar limit by Kazakov-Kostov.

Wilson loop with self-intersection

N=64

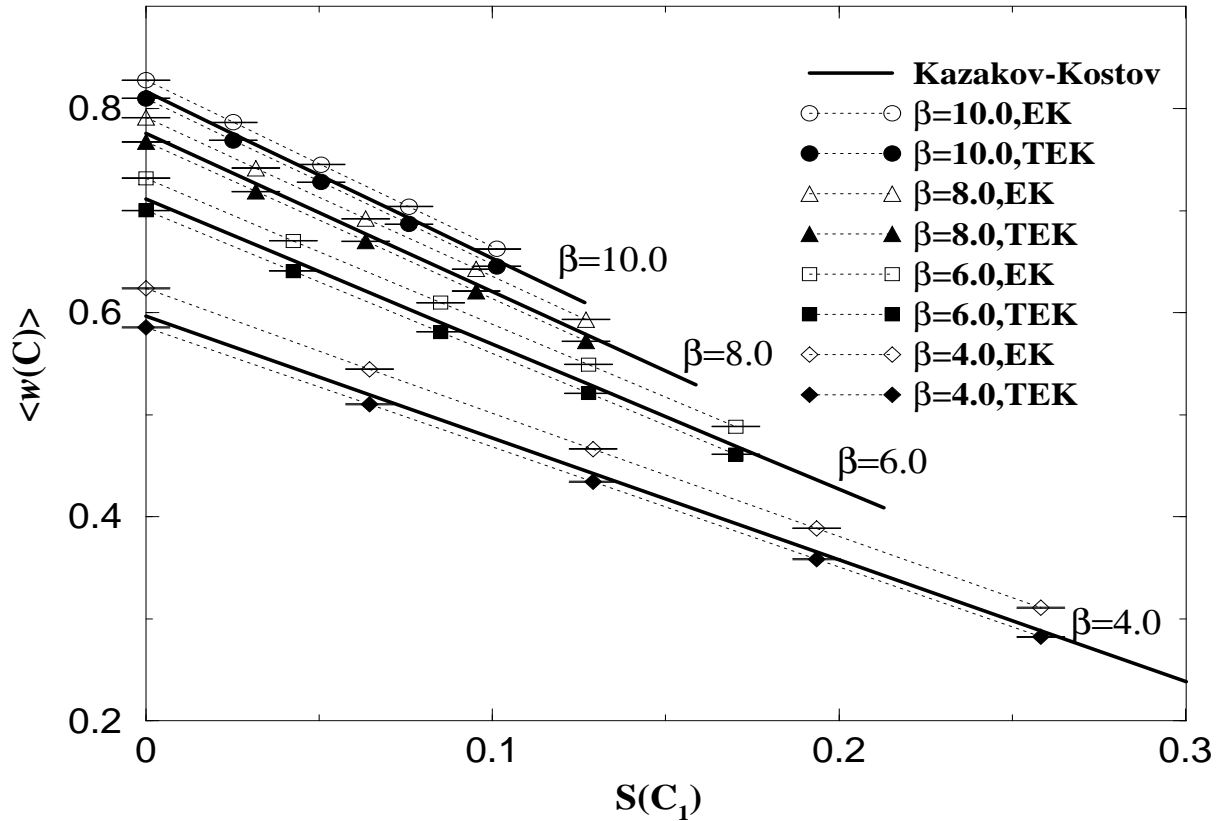


Figure 8: The expectation value of $w(C)$ in the EK (open symbols) and the TEK model (filled symbols) for $N = 64$ with $\beta = 4.0$ (diamonds), 6.0 (squares), 8.0 (triangles) and 10.0 (circles) are plotted against the physical area $S(C_1) = a^2 LL_1$. The straight heavy solid lines represent the continuum results in the planar limit by Kazakov-Kostov.

a unit vector in the α direction. Note that the observables (2.5) considered in the previous section can be viewed as the Wilson loops in the EK model with $n_\mu = 0$, while in this section we consider those with $n_\mu \neq 0$ as well. After the T-duality transformation, the winding of the Wilson loops represents the momentum distribution of the string in the two-dimensional space time. The total physical momentum carried by the string which corresponds to the Wilson loop (4.1) is given by $P_\mu = n_\mu a$. Under the $U(1)^2$ transformation (2.2), the Wilson loop (4.1) is multiplied by $\exp(in_\mu\theta_\mu)$. Since the symmetry is not spontaneously broken in the present model, the one-point function of Wilson loops in the winding sector should vanish. Similarly, the n -point function should vanish in general, unless the sum of the winding number of the Wilson loops is zero. After the T-duality transformation, the above selection rule gives nothing but the momentum conservation in the two-dimensional space time. This corresponds to the fact that the $U(1)^2$ symmetry is nothing but the translational invariance when we identify the phase of the eigenvalues of U_μ as the two-dimensional space-time coordinates.

In what follows, we consider

$$\begin{aligned} O_{\alpha\beta}^{(n)}(L) &= \text{tr}(U_\alpha^L U_\beta^L U_{-\alpha}^L U_{-\beta}^L) \\ O_\alpha^{(w)}(L) &= \text{tr}(U_\alpha^L), \end{aligned} \quad (4.2)$$

which give typical Wilson loops in the non-winding sector and the winding sector respectively. Due to the trace, the independent operators in the non-winding sector are actually given by $O_{12}^{(n)}(L)$ and $O_{21}^{(n)}(L)$, which are complex conjugate to each other. When we take the $a \rightarrow 0$ limit, we have to send L to the infinity by fixing aL . Note that in (4.1) and (4.2), we do not put $1/N$ in front of the trace as we did in (2.5). This is because with this convention, the power counting of N for correlation functions matches with the one conventional in the old-fashioned matrix model [1].

We do not consider the TEK model in what follows, since the interpretation as a string theory is not as obvious as in the EK model. Indeed, as is seen in Fig. 5, the TEK model does not show any systematic finite N effects, while the EK model does. It is therefore natural to consider that the TEK model does not allow any sensible double scaling limit.

Let us first examine the one-point function of Wilson loops in the non-winding sector, namely $G_1^{(n)}(L) = \langle O_{12}^{(n)}(L) \rangle$. The observable $\langle w(L \times L) \rangle$ considered in the previous section is nothing but $N^{-1}G_1^{(n)}(L)$. We have seen in Fig. 3 how the data for $N^{-1}G_1^{(n)}(L)$ approach the planar limit when we increase N with fixed β . In Fig. 9, we plot $N^{-1}G_1^{(n)}(L)$ against

one-point function in the non-winding sector

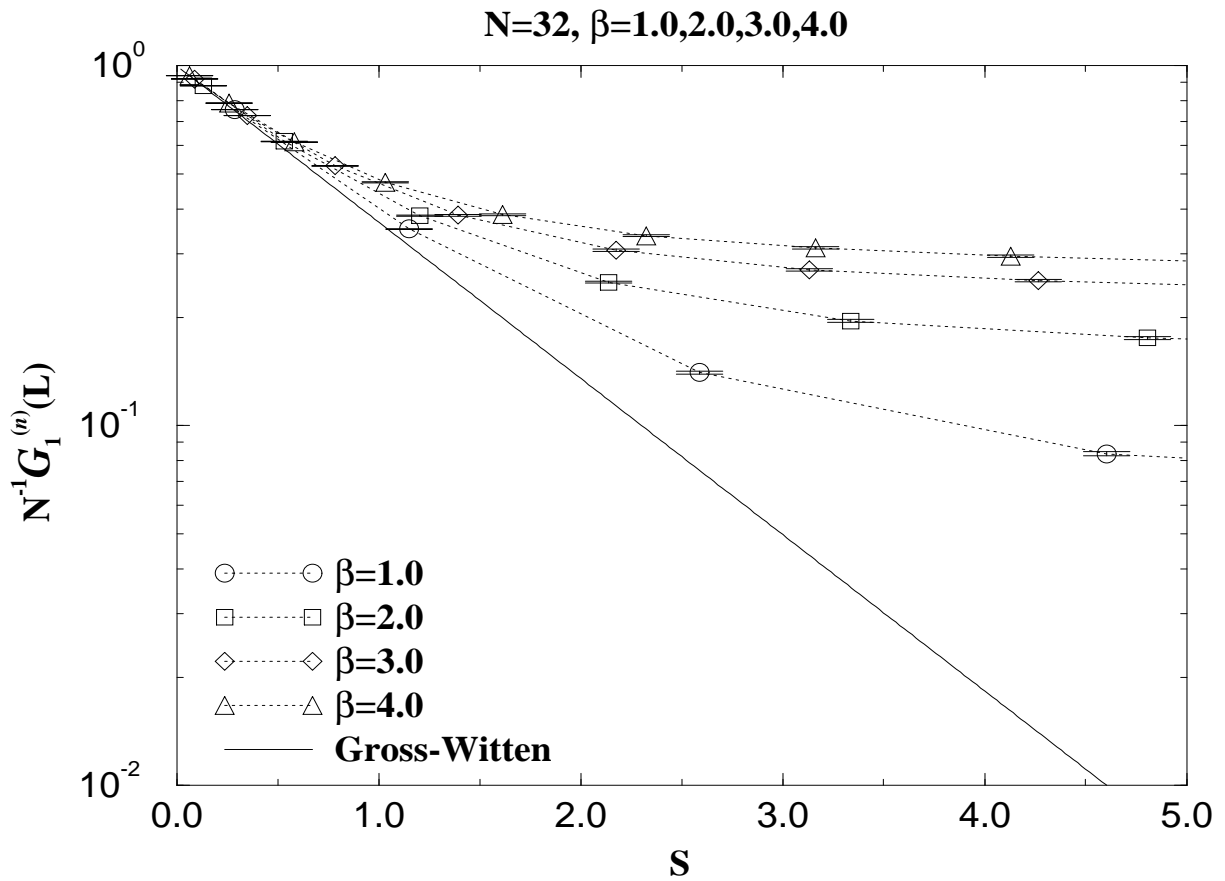


Figure 9: The one-point function of the Wilson loops in the non-winding sector $N^{-1}G_1^{(n)}(L)$ in the EK model is plotted against $S = (aL)^2$ for $N = 32$ with $\beta = 1.0$ (circles), 2.0 (squares), 3.0 (diamonds) and 4.0 (triangles). The straight solid line represents the planar result by Gross-Witten.

$S = (aL)^2$ for fixed N with various values of β . One can see that the effect of increasing β is quite similar to the finite N effect. Thus it is natural to expect that we may be able to balance these two effects by taking the limit $\beta \rightarrow \infty$ together with the $N \rightarrow \infty$ limit. Indeed we find that $N^{-1}G_1^{(n)}(L)$ scales in the large N limit by fixing β/N . In Fig. 10 we show the data for $\beta/N = 1.0/32$ and $\beta/N = 1.5/32$. N is taken to be 32, 48, 64, 96 and 128. We see a clear scaling behavior. Measurements have been done every 10 sweeps and we average over 2000 configurations for $N = 32 \sim 96$, and over 1000 configurations for $N = 128$. All the data in this section have been obtained in this way, unless mentioned.

The finite N effect is seen as a deviation from the scaling behavior for large S . The deviation shows up at $L \simeq N/8$. Since $a \propto 1/\sqrt{\beta} \propto 1/\sqrt{N}$ for large N , the scaling region enlarges as \sqrt{N} . The scaling function for fixed β/N approaches the planar limit as β/N becomes smaller.

From this observation, it is natural to expect that the double scaling limit of the EK model can be taken by fixing β/N , which corresponds to the string coupling constant g_{str} . The planar limit corresponds to $g_{str} = 0$.

Let us next consider Wilson loops in the winding sector. Since the one-point function vanishes as is explained above, we consider the two-point function

$$G_2^{(w)}(L) = \langle O_\mu^{(w)}(L) O_{-\mu}^{(w)}(L) \rangle. \quad (4.3)$$

Note that the right hand side does not depend on μ , due to the rotational invariance. In the measurement, we average over $\mu = 1, 2$ to increase the statistics. This quantity is naively $\mathcal{O}(N^2)$, but due to the factorization, its leading term is given by $\langle O_\mu^{(w)}(L) \rangle \langle O_{-\mu}^{(w)}(L) \rangle$, which actually vanishes due to the $U(1)^2$ symmetry. The order of the quantity is therefore $\mathcal{O}(1)$. We can regard the $\mathcal{O}(1)$ quantity as the connected two-point function of the Wilson loops in the winding sector.

Let us examine if the two-point function $G_2^{(w)}(L)$ allows the double scaling limit. In Fig. 11, we plot $G_2^{(w)}(L)$ against $l = aL$ for $\beta/N = 1.0/32$ with $N = 32, 48, 64, 96$ and 128. No scaling behavior is observed. However, as is the case with the double scaling limit in the old-fashioned matrix models [1], we might have to admit the wave function renormalization. Since the Fig. 11 is a log-log plot, the wave function renormalization amounts to shifting the curves relatively along the vertical axis. Fig. 12 shows the result for the renormalized two-point function

$$\tilde{G}_2^{(w)}(L) = \beta^{-0.65} G_2^{(w)}(L). \quad (4.4)$$

one-point function in the non-winding sector

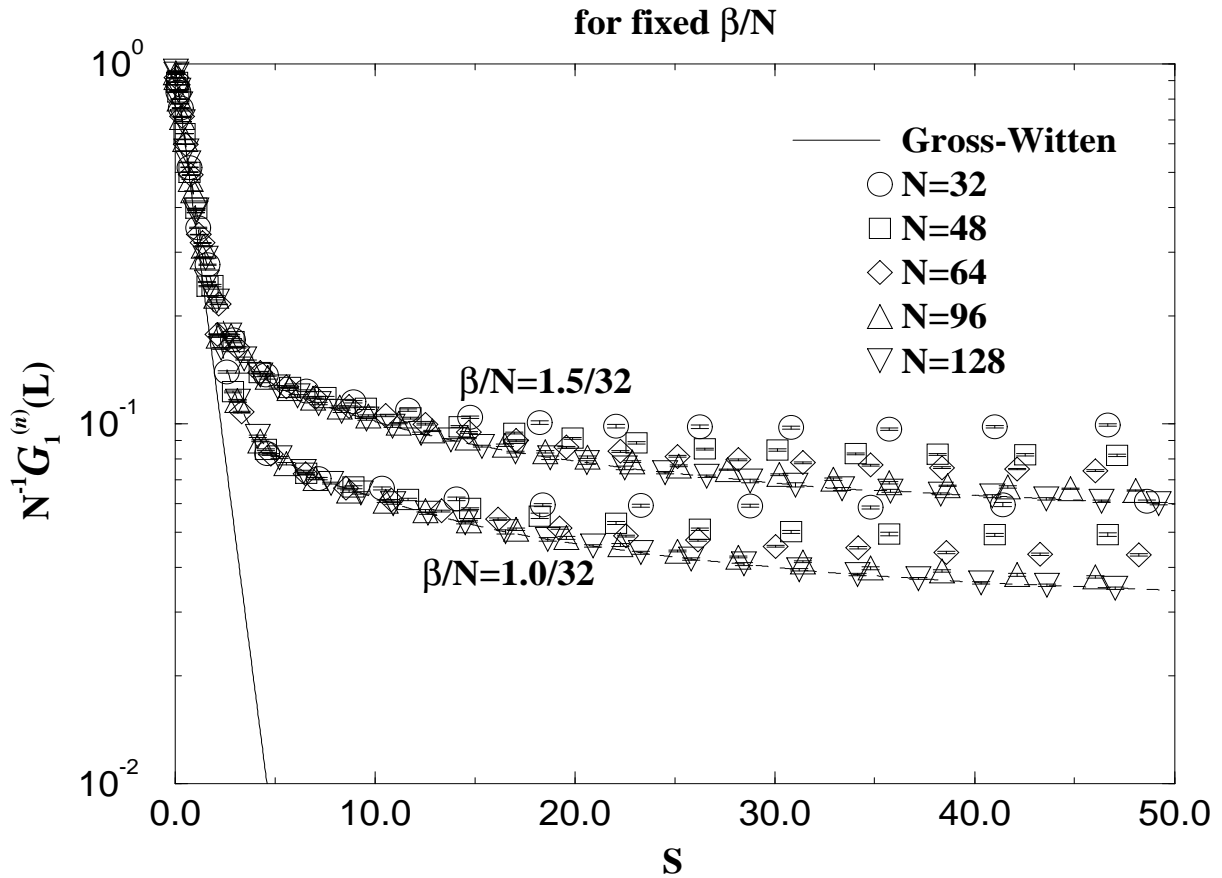


Figure 10: The one-point function of the Wilson loops in the non-winding sector $N^{-1}G_1^{(n)}(L)$ in the EK model is plotted against $S = (aL)^2$ for the sets of β and N with β/N fixed to $1.0/32$ and $1.5/32$. Each symbol represents the data for $N = 32$ (circles), $N = 48$ (squares), $N = 64$ (diamonds), $N = 96$ (triangles) and $N = 128$ (inverse triangles). The straight solid line represents the planar result by Gross-Witten. The dashed lines, which connect the data for $N = 128$, are drawn to guide the eye.

One can see a clear scaling behavior in the intermediate region of l . The scaling function is a power of l for large l , and the power is 0.80(2). The finite N effect can be seen as a saturation of the power-law behavior in the large l region, which shows up at $L \simeq N$. This is to be compared with the case with $N^{-1}G_1^{(n)}(L)$ in Fig. 10, where the deviation from the scaling behavior in the large l region shows up at $L \simeq N/8$. This discrepancy is not strange since the meaning of L depends on which of the two operators $O_{\alpha\beta}^{(n)}(L)$ and $O_\alpha^{(w)}(L)$ one considers.

Unlike in Fig. 10, there is a deviation from the scaling behavior also in the small l region. The tendency of convergence to a scaling function in this region is not clearly seen up to $N = 128$. The fact that such a deviation does not appear for $N^{-1}G_1^{(n)}(L)$ in Fig. 10 might be rather considered as an accidental property of the Wilson loop in the non-winding sector.

We can see the scaling behavior for different β/N as well. In Fig. 13, we plot the renormalized two-point function $\tilde{G}_2^{(w)}(L)$ against $l = aL$ for $\beta/N = 1.5/32$ with $N = 32, 48, 64, 96$ and 128. The behavior is qualitatively the same as that of Fig. 12. Note that this result shows that the wave function renormalization does not depend on $g_{str} = \beta/N$, which is to be expected. The power of the scaling function in the large l region is 0.72(3).

In order to understand the power-law behavior, we calculate $G_2^{(w)}(L)$ for $\beta = 0$ in the large N limit analytically through Schwinger-Dyson equation ². We consider the quantity $\langle \text{tr}(t^a U_\mu^L) \text{tr}(U_\mu^{\dagger L}) \rangle$, where t^a ($a = 1, \dots, N^2$) denote the generators of the $U(N)$ group. By changing the variable of integration as $U_\mu \rightarrow (1 - i\epsilon t^a)U_\mu$, we obtain the following identity.

$$\sum_{M=1}^L \langle \text{tr}(t^a U_\mu^{L-M} t^a U_\mu^M) \text{tr}(U_\mu^{\dagger L}) \rangle - L \langle \text{tr}(t^a U_\mu^L) \text{tr}(t^a U_\mu^{\dagger L}) \rangle = 0 \quad (4.5)$$

Taking a summation over $a = 1, \dots, N^2$, we obtain

$$N \langle \text{tr}(U_\mu^L) \text{tr}(U_\mu^{\dagger L}) \rangle + \sum_{M=1}^{L-1} \langle \text{tr}(U_\mu^{L-M}) \text{tr}(U_\mu^M) \text{tr}(U_\mu^{\dagger L}) \rangle - NL = 0, \quad (4.6)$$

where we have used the identity $\sum_a (t^a)_{ij} (t^a)_{kl} = \delta_{il} \delta_{jk}$. Since the three-point function $\langle \text{tr}(U_\mu^{L-M}) \text{tr}(U_\mu^M) \text{tr}(U_\mu^{\dagger L}) \rangle$ is at most $\mathcal{O}(1/N)$ as we explain later, we obtain

$$G_2^{(w)}(L) = \langle \text{tr}(U_\mu^L) \text{tr}(U_\mu^{\dagger L}) \rangle = L. \quad (4.7)$$

We have checked this result explicitly by Monte Carlo simulation. It is natural to expect that in the planar limit the two-point function in the large l region can be described by the

²We thank H. Kawai for suggesting the use of Schwinger-Dyson equation for this purpose.

two-point function in the winding sector without wave function renormalization

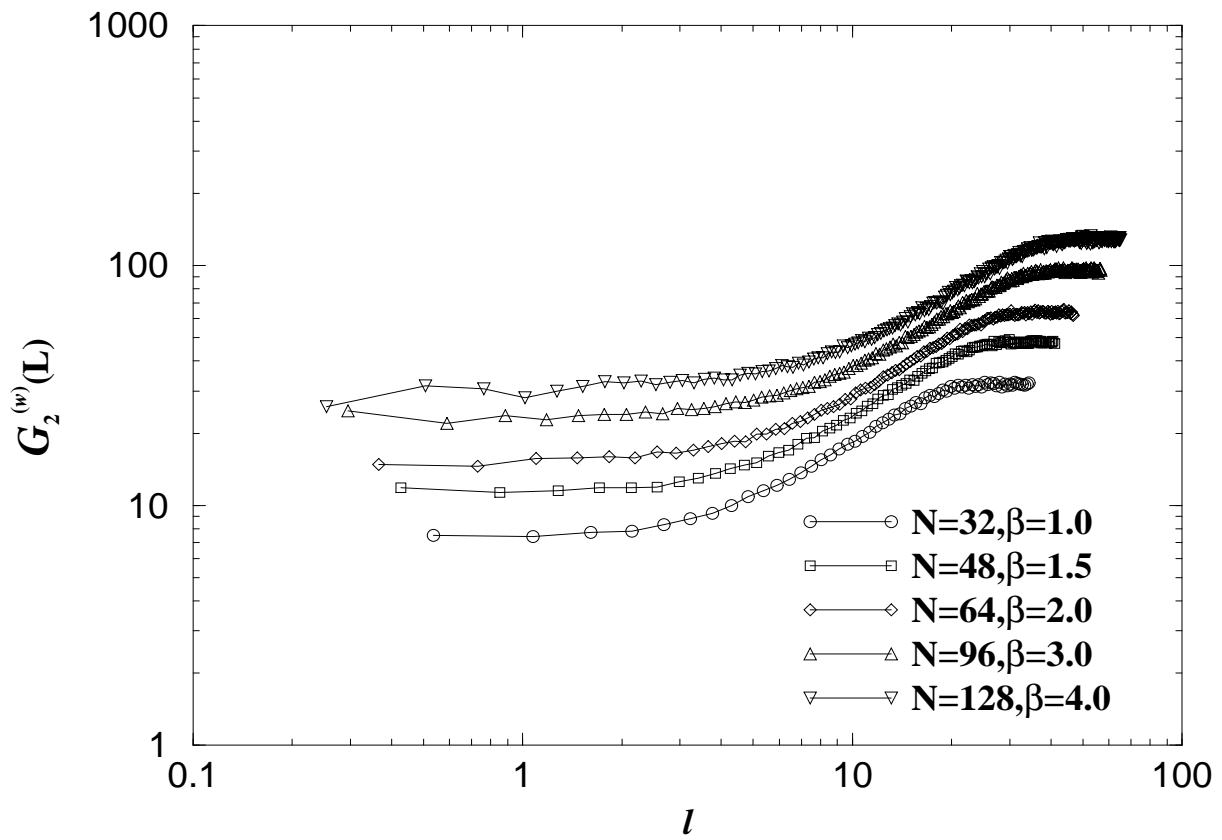


Figure 11: The two-point function in the winding sector without the wave function renormalization $G_2^{(w)}(L)$ is plotted against $l = aL$ for sets of β and N with $\beta/N = 1.0/32$. Each symbol represents the data for $N = 32$ (circles), $N = 48$ (squares), $N = 64$ (diamonds), $N = 96$ (triangles) and $N = 128$ (inverse triangles).

two-point function in the winding sector with wave function renormalization

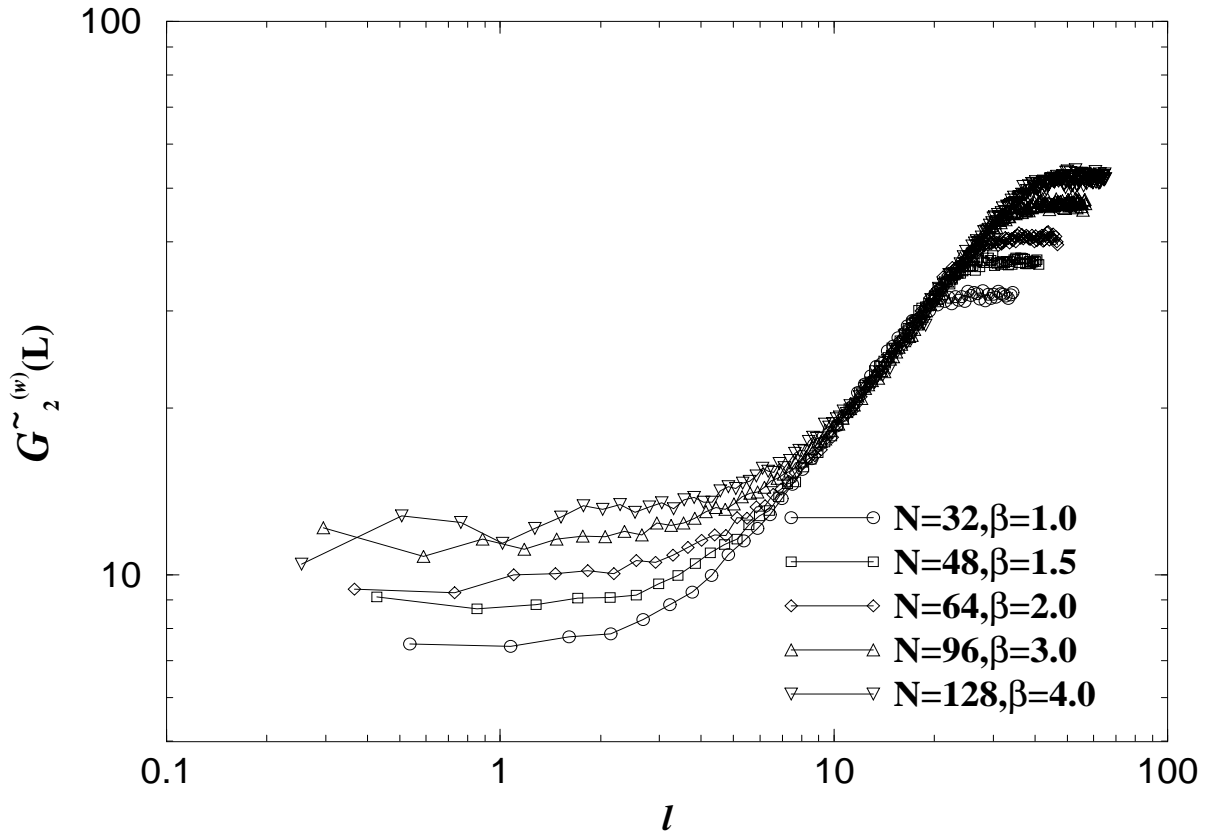


Figure 12: The two-point function in the winding sector with the wave function renormalization $\tilde{G}_2^{(w)}(L)$ is plotted against $l = aL$ for sets of β and N with $\beta/N = 1.0/32$. Each symbol represents the data for $N = 32$ (circles), $N = 48$ (squares), $N = 64$ (diamonds), $N = 96$ (triangles) and $N = 128$ (inverse triangles).

two-point function in the winding sector with wave function renormalization

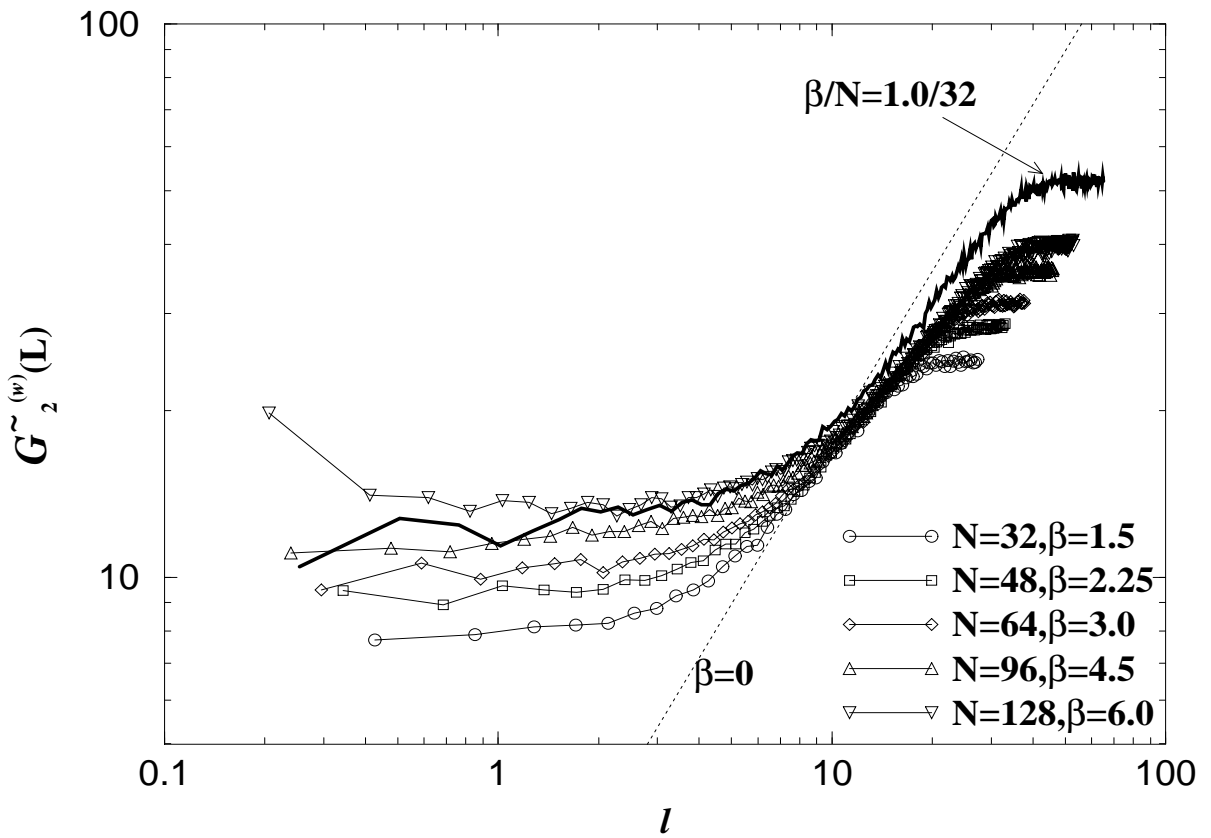


Figure 13: The two-point function in the winding sector with the wave function renormalization $\tilde{G}_2^{(w)}(L)$ is plotted against $l = aL$ for sets of β and N with $\beta/N = 1.5/32$. Each symbol represents the data for $N = 32$ (circles), $N = 48$ (squares), $N = 64$ (diamonds), $N = 96$ (triangles) and $N = 128$ (inverse triangles). The result for $\beta/N = 1.0/32$ with $N = 128$ are replotted by the heavy line. The dotted line is a line with slope 1, which represents the result for $\beta = 0$ and $N = \infty$.

strong coupling limit obtained above. The fact that the power of l in the scaling function approaches one for decreasing $g_{str} = \beta/N$ can be naturally understood in this way.

Note that the wave function renormalization was actually necessary for $G_1^{(n)}(L)$ as well, since we had to multiply it by N^{-1} when we see the scaling behavior. In this sense, we should say that the renormalized one-point function is given by $\tilde{G}_1^{(n)}(L) = \beta^{-1}G_1^{(n)}(L)$. Thus, although the result for the two-point function of the Wilson loops in the winding sector supports to some extent our conjecture concerning the existence of the double scaling limit, we encounter a new problem: why the wave function renormalization for the one-point function $G_1^{(n)}(L)$ is not equal to that for the two-point function $G_2^{(w)}(L)$.

In order to clarify this problem, we consider the two-point function of Wilson loops in the non-winding sector defined by $\langle O_{12}^{(n)}(L)O_{12}^{(n)}(L) \rangle$ and $\langle O_{12}^{(n)}(L)O_{21}^{(n)}(L) \rangle$. These observables are $\mathcal{O}(N^2)$ quantity, but the leading term is given by the disconnected part $\langle O_{12}^{(n)}(L) \rangle \langle O_{12}^{(n)}(L) \rangle$ and $\langle O_{12}^{(n)}(L) \rangle \langle O_{21}^{(n)}(L) \rangle$, respectively, due to the factorization. The connected two-point function can be defined by

$$\langle O_{12}^{(n)}(L)O_{12}^{(n)}(L) \rangle_c = \langle O_{12}^{(n)}(L)O_{12}^{(n)}(L) \rangle - \langle O_{12}^{(n)}(L) \rangle \langle O_{12}^{(n)}(L) \rangle \quad (4.8)$$

$$\langle O_{12}^{(n)}(L)O_{21}^{(n)}(L) \rangle_c = \langle O_{12}^{(n)}(L)O_{21}^{(n)}(L) \rangle - \langle O_{12}^{(n)}(L) \rangle \langle O_{21}^{(n)}(L) \rangle, \quad (4.9)$$

which are $\mathcal{O}(1)$ quantities.

Since $\langle O_{12}^{(n)}(L) \rangle = \langle O_{21}^{(n)}(L) \rangle \in \mathcal{R}$, as is mentioned in the previous section, we can avoid the subtraction by considering the difference of the two-point functions.

$$G_2^{(n)-}(L) \equiv \frac{1}{2} \{ \langle O_{12}^{(n)}(L)O_{21}^{(n)}(L) \rangle_c - \langle O_{12}^{(n)}(L)O_{12}^{(n)}(L) \rangle_c \} \quad (4.10)$$

$$= \frac{1}{2} \{ \langle O_{12}^{(n)}(L)O_{21}^{(n)}(L) \rangle - \langle O_{12}^{(n)}(L)O_{12}^{(n)}(L) \rangle \} \quad (4.11)$$

$$= \langle (\text{Im}O_{12}^{(n)}(L))^2 \rangle. \quad (4.12)$$

We have used the fact that $\langle O_{12}^{(n)}(L)O_{12}^{(n)}(L) \rangle = \langle O_{12}^{(n)}(L)O_{21}^{(n)}(L) \rangle \in \mathcal{R}$ in the third equality. In Fig. 14 we plot the $G_2^{(n)-}(L)$ against $S = (aL)^2$ for $\beta/N = 1.0/32$ with $N = 32, 48, 64, 96$ and 128. There seems to be no scaling behavior. Let us assume the same wave function renormalization as the one for $G_2^{(w)}(L)$ in (4.4). In Fig. 15, we plot $\tilde{G}_2^{(n)-}(L) = \beta^{-0.65}G_2^{(n)-}(L)$ for $\beta/N = 1.0/32$ with $N = 32, 48, 64, 96$ and 128. We find a clear scaling behavior. The discrepancy in the large S region starts from $L \simeq N/8$, which is the same as with $\tilde{G}_1^{(n)}(L)$. This suggests that the operator $O_{\alpha\beta}^{(n)}(L)$ gives a finite N effect to the correlation function which includes it for $L \simeq N/8$ in general. It is natural to expect that this is the case also

two-point function in the non-winding sector without wave function renormalization

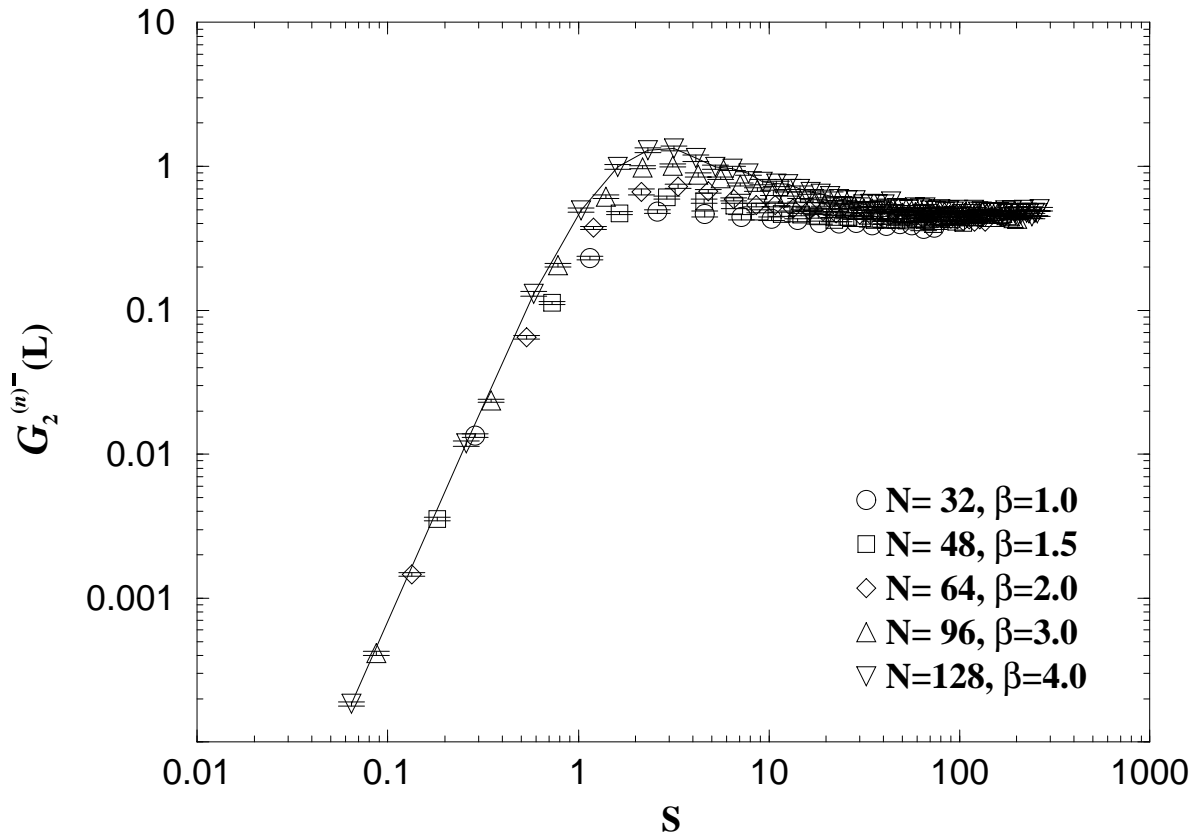


Figure 14: The two-point function in the non-winding sector without the wave function renormalization $G_2^{(n)-}(L)$ is plotted against $S = (aL)^2$ for sets of β and N with $\beta/N = 1.0/32$. Each symbol represents the data for $N = 32$ (circles), $N = 48$ (squares), $N = 64$ (diamonds), $N = 96$ (triangles) and $N = 128$ (inverse triangles). The solid line, which connects the data for $N = 128$, is drawn to guide the eye.

two-point function in the non-winding sector with wave function renormalization

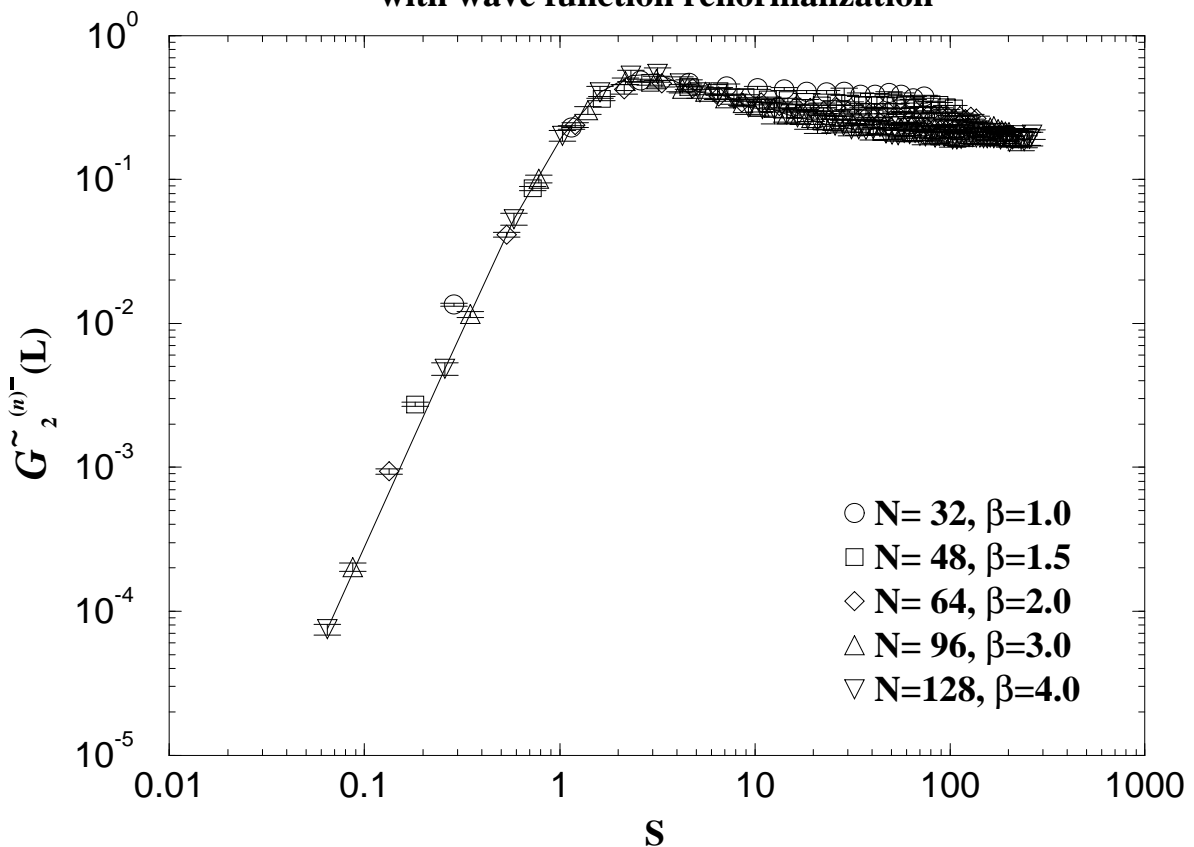


Figure 15: The two-point function in the non-winding sector with the wave function renormalization $\tilde{G}_2^{(n)-}(L)$ is plotted against $S = (aL)^2$ for sets of β and N with $\beta/N = 1.0/32$. Each symbol represents the data for $N = 32$ (circles), $N = 48$ (squares), $N = 64$ (diamonds), $N = 96$ (triangles) and $N = 128$ (inverse triangles). The solid line, which connects the data for $N = 128$, is drawn to guide the eye.

with the operator $O_\alpha^{(w)}(L)$ with $L \simeq N$, which we exploit in discussing the scaling behavior of the three-point function of Wilson loops in the winding sector later. The scaling seems to extend to the small l region except for the data that corresponds to $L = 1$. This is consistent with our previous observation that the Wilson loops in the non-winding sector do not suffer from finite N effects in the small l region, unlike those in the winding sector.

Similarly, we can define

$$G_2^{(n)+}(L) \equiv \frac{1}{2} \left\{ \langle O_{12}^{(n)}(L) O_{12}^{(n)}(L) \rangle_c + \langle O_{12}^{(n)}(L) O_{21}^{(n)}(L) \rangle_c \right\} \quad (4.13)$$

$$= \langle (\text{Re} O_{12}^{(n)}(L))^2 \rangle - \langle O_{12}^{(n)}(L) \rangle^2. \quad (4.14)$$

The result for $\tilde{G}_2^{(n)+}(L) = \beta^{-0.65} G_2^{(n)+}(L)$ also shows the scaling behavior, which is qualitatively the same as in Fig. 15, albeit larger error bars due to the subtraction.

As in the case of $G_2^{(w)}(L)$, we can calculate $G_2^{(n)\pm}(L)$ for $\beta = 0$ in the large N limit by using the Schwinger-Dyson equation and obtain $G_2^{(n)\pm}(L) = 1/2$. This suggests that in the planar limit, the asymptotic behavior of the scaling function of $G_2^{(n)\pm}(L)$ for large l is constant, which is consistent with our results.

From these observations, we conclude that only the one-point function is exceptional concerning the wave function renormalization. Note that the wave function renormalization of $G_1^{(n)}(L)$ is, in some sense, kinematically constrained by the fact that $G_1^{(n)}(0) = N$. The non-vanishing one-point function can be considered as the background of the corresponding string field and the exceptional behavior is not very unnatural.

As a further check of the existence of the double scaling limit, we consider the three-point function of Wilson loops in the winding sector defined by

$$G_3^{(w)}(L) = \langle O_\mu^{(w)}(L) O_\mu^{(w)}(L) O_{-\mu}^{(w)}(2L) \rangle. \quad (4.15)$$

Note that the right hand side does not depend on μ , and we average over $\mu = \pm 1, \pm 2$ in the measurement to order to increase the statistics. The three-point function is naively $\mathcal{O}(N^3)$ quantity, but the leading term $\langle O_\mu^{(w)}(L) \rangle \langle O_\mu^{(w)}(L) \rangle \langle O_{-\mu}^{(w)}(2L) \rangle$ and the subleading term $\langle O_\mu^{(w)}(L) O_\mu^{(w)}(L) \rangle \langle O_{-\mu}^{(w)}(2L) \rangle$ etc., which are of order $\mathcal{O}(N)$, vanish due to the $U(1)^2$ symmetry, and it is actually $\mathcal{O}(1/N)$ quantity, which can be regarded as the connected three-point function.

In Fig. 16 and Fig. 17, we plot $G_3^{(w)}(L)$ and $\tilde{G}_3^{(w)}(L) = (\beta/4.0)^{-0.65 \times 3/2} G_3^{(w)}(L)$, respectively, against $l = aL$ for $\beta/N = 1.0/32$ with $N = 32, 48, 64, 96$ and 128 . Measurements have been done every 10 sweeps. Each point is an average over 4000 configurations for

three-point function in the winding sector

without wave function renormalization

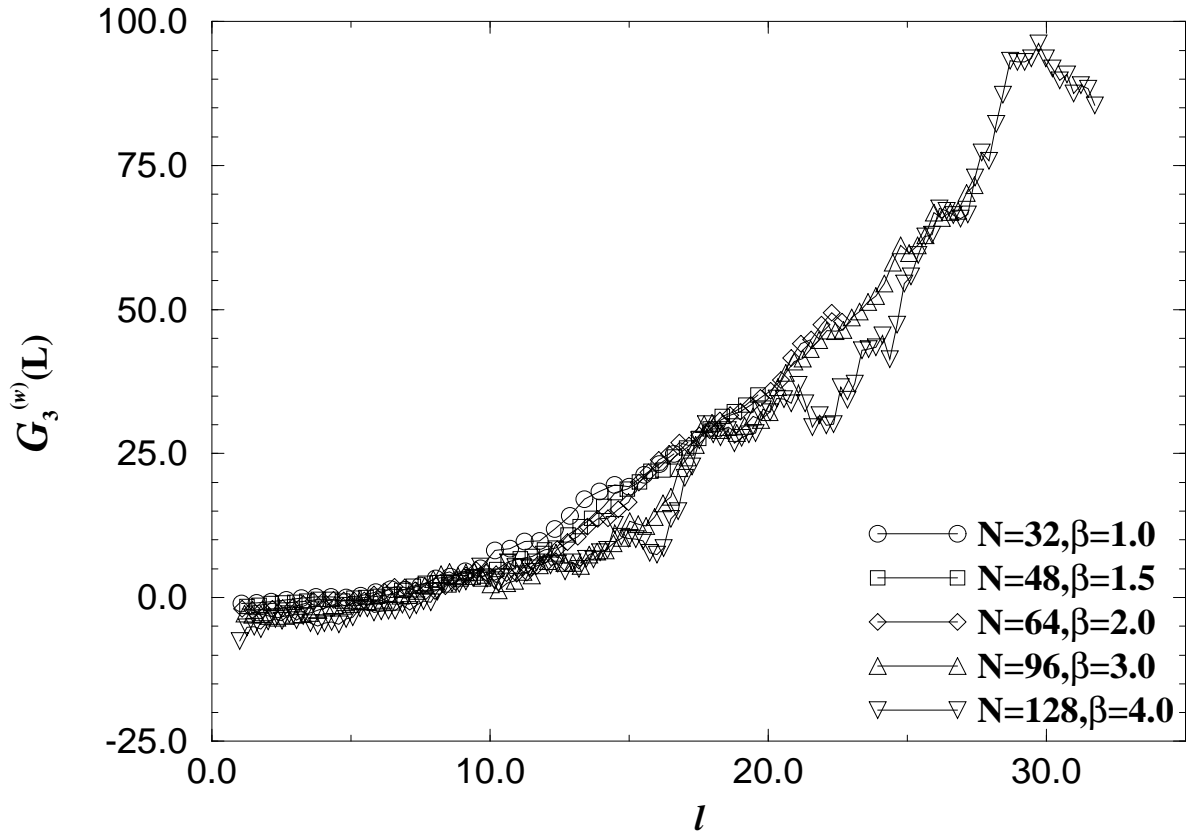


Figure 16: The three-point function in the winding sector without the wave function renormalization $G_3^{(w)}(L)$ is plotted against $l = aL$ for sets of β and N with $\beta/N = 1.0/32$. Each symbol represents the data for $N = 32$ (circles), $N = 48$ (squares), $N = 64$ (diamonds), $N = 96$ (triangles) and $N = 128$ (inverse triangles).

three-point function in the winding sector

with wave function renormalization

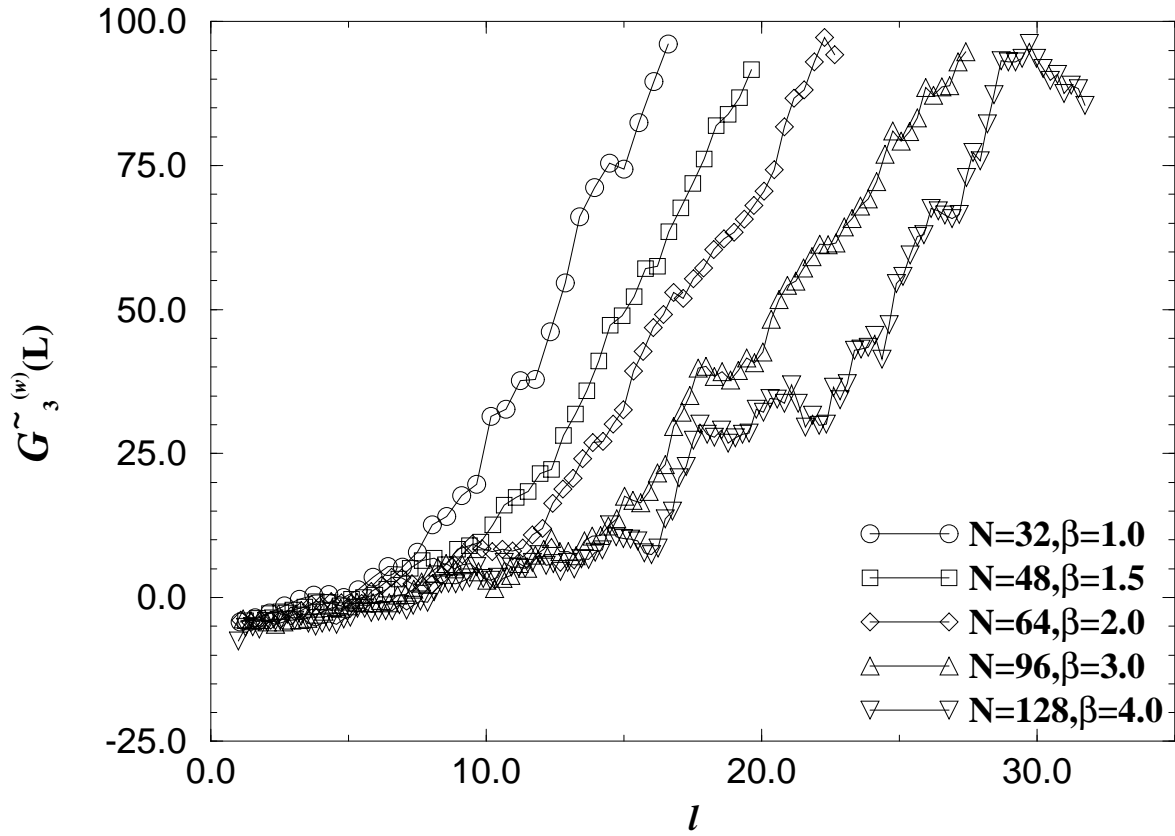


Figure 17: The three-point function in the winding sector with the wave function renormalization $\tilde{G}_3^{(w)}(L)$ is plotted against $l = aL$ for sets of β and N with $\beta/N = 1.0/32$. Each symbol represents the data for $N = 32$ (circles), $N = 48$ (squares), $N = 64$ (diamonds), $N = 96$ (triangles) and $N = 128$ (inverse triangles).

$N = 32 \sim 96$, and over 2000 configurations for $N = 128$. Note that since the data can be both positive and negative, we cannot make a log plot, though we should do so when we discuss scaling behaviors. In order to avoid a possible unfair comparison of the figures, we have defined the $\tilde{G}_3^{(w)}(L)$ so that the data for $N = 128$ look the same as those for $G_3^{(w)}(L)$. Although the data are too noisy to confirm the scaling behavior exclusively with the particular wave function renormalization assumed here, the renormalized data are at least consistent with the scaling behavior in some region of l . Furthermore, the deviation from the scaling in the large l region shows up at $2L \simeq N$, which is in agreement with the finite N effects seen for the two-point function of the same operator, namely $\tilde{G}_2^{(w)}(L)$. This is not the case with the data without the wave function renormalization. We therefore conclude that the data for the three-point function also support the existence of the double scaling limit with the universal wave function renormalization.

5 Conclusion and discussion

In this paper, we studied the EK model as a toy model of the IIB matrix model. In the planar limit, the one-point function of the Wilson loops in the non-winding sector gives the expectation value of Wilson loops in the large N lattice gauge theory in two dimensions. Using the exact results in the 2D large N lattice gauge theory, we fixed how to send a to 0 as we send β to infinity as

$$a = \sqrt{-\log \left(1 - \frac{1}{4\beta}\right)}. \quad (5.1)$$

In the planar limit, N is sent to infinity before taking the limit $a \rightarrow 0$ and $\beta \rightarrow \infty$. We found that there is another way of taking the large N limit, namely with β/N fixed. We found that the correlation functions of Wilson loops in the non-winding sector as well as in the winding sector have nontrivial limits with the wave function renormalization $\beta^{-0.65/2}$ for each Wilson loop. The only exception we saw is the one-point function, for which the wave function renormalization is β^{-1} . We consider that this is not so unnatural, since the one-point function is special in the sense it can be considered as the non-vanishing background of the corresponding string field.

The deviation from the scaling behavior due to the finite N is seen in the large l region. The number of the links for which the Wilson loop operator gives finite N effects depends on the operator considered. It is around N for the Wilson loops in the winding sector and

around $N/2$ for the Wilson loops in the non-winding sector. In either case, the physical scaling region enlarges as \sqrt{N} in the large l region.

On the other hand, the situation in the small l region is not so clear. The deviation from the scaling behavior is seen for the two-point functions of Wilson loops in the winding sector. Convergence to a scaling function seems to be slow. For the correlation functions of the Wilson loops in the non-winding sector, on the other hand, no significant deviation from the scaling behavior is seen in the small l region. We consider this as an accidental property of Wilson loops in the non-winding sector.

The data for the n -point functions with $n \geq 3$ are unfortunately too noisy to confirm the scaling behavior for fixed β/N . We found, however, that the data for the three-point function of Wilson loops in the winding sector with the same wave function renormalization are consistent with the scaling. Furthermore, the deviation from the scaling in the large l region due to the finite N effects appears in a manner which is consistent with the finite N effects seen for the two-point function of the same operator.

We calculated the two-point functions for $\beta = 0$ in the large N limit by using the Schwinger-Dyson equation. The result seems to describe the large l behavior of the corresponding quantity in the planar limit. We can calculate the connected n -point functions in general, which are order $\mathcal{O}(1/N^{(n-2)})$ quantities. We find that the coefficient of $1/N^{(n-2)}$ is zero for $\beta = 0$ in the large N limit. This suggests that the n -point functions with $n \geq 3$ in the planar limit goes to zero in the large l region. One might fear that the string theory constructed through the double scaling limit of the EK model is a free theory. Our data suggest, however, that the three-point function is not constantly zero at least when $g_{str} \neq 0$.

A technically important comment is that while the old-fashioned matrix model, whose action is unbounded from below, becomes well-defined only in the large N limit, the EK model as well as the IIB matrix model is completely well-defined even for a finite N . This makes these models much easier to study numerically than the old-fashioned matrix model.

To summarize, our numerical results suggest strongly that the double scaling limit of the EK model can be taken by sending N to the infinity with the following combinations of parameters fixed.

$$\beta/N \sim g_{str} \quad (5.2)$$

$$Na^2 \sim (\alpha' g_{str})^{-1}, \quad (5.3)$$

where g_{str} is the string coupling constant and α' is the string tension.

It is intriguing to ask what is the string theory constructed through the double scaling limit of the EK model. We interpreted the model as a string theory through the T-duality transformation as is done in the IIB matrix model. The target space is therefore two-dimensional space time compactified to a torus of size $\sim 1/a$, which goes to infinity as $a \rightarrow 0$. The theory must be different from the $c = 1$ matrix model interpreted as 2D string theory with linear dilaton background, since we have at least the discrete rotational invariance in the EK model. Note also that although the target space is two-dimensional, the dynamical degrees of freedom of the link variables are actually absorbed by the gauge degrees of freedom. It might be that this theory cannot be described as 2D gravity coupled to some conformal matter.

An important difference between the EK model and the IIB matrix model is that the dynamical variables in the former are the unitary matrices, while those in the latter are the hermitian matrices. Considering the interpretation of the models as string theories using the T-duality transformation, it seems to be more natural to formulate the matrix models in terms of unitary matrices. Constructing such a formulation for type IIB superstring has been considered in Ref. [22]. The problem corresponding to the fermion doublers in the lattice chiral gauge theory has been overcome by the use of the overlap formalism, but the remaining problem is whether one can recover the supersymmetry in the large N limit with the proposed model or with fine-tuning of the coefficients of some possible counterterms. On the other hand, one could consider a hermitian matrix version of the two-dimensional EK model, with the action $S = -\frac{1}{4g^2} \text{tr}[A_\mu, A_\nu]^2$, but the theory is not well defined [23]. We can make the theory well defined, for example, by adding a term like $m^2(\text{tr}A_\mu^2 - \frac{1}{N}(\text{tr}A_\mu)^2)$, which preserves the $U(1)^2$ symmetry : $A_\mu \rightarrow A_\mu + \alpha_\mu$. However, the $U(1)^2$ symmetry is then spontaneously broken and the model must be in a universality class other than the one corresponding to the two-dimensional EK model.

Despite the above subtlety, the relations (5.2) and (5.3) which specify how one should take the double scaling limit in the two-dimensional EK model might be naively compared with the ones conjectured for the IIB matrix model [10]; namely,

$$g^2 N \sim \alpha'^2 \quad (5.4)$$

$$N\epsilon^2 \sim g_{str}^{-1}. \quad (5.5)$$

ϵ is a dimensionless constant which corresponds naively to a . We therefore have $a \sim \epsilon \alpha'^{-1/2}$. This means that the relation (5.5) coincides with the corresponding one in the EK model,

namely (5.3). The coupling constant g can be related to β naively in the following way. We relate the hermitian matrices A_μ in the IIB matrix model to the link variables U_μ in the EK model through $U_\mu = \exp(iaA_\mu)$, and expand the action (2.1) in terms of a . We obtain $S = -N\beta a^4 \text{tr}[A_\mu, A_\nu]^2 \dots$. In Ref. [10], the factor in front of the trace is denoted as $1/4g^2$, which means that $1/g^2 \sim N\beta a^4$. Therefore, (5.4) corresponds naively to fixing β/N^2 in our notation.

The fact that a sensible double scaling limit can be taken for the large N reduced model of two-dimensional lattice gauge theory is itself encouraging for the research of nonperturbative formulation of superstring theory through the IIB matrix model. We hope to report on numerical studies of the IIB matrix model in future publications.

Acknowledgments

We would like to thank H. Kawai for continuous encouragements and for stimulating discussions. The authors are also grateful to M. Fukuma, V.A. Kazakov and A. Tsuchiya for valuable comments. This work is supported by the Supercomputer Project (No.97-18) of High Energy Accelerator Research Organization (KEK).

References

- [1] E. Brézin and V.A. Kazakov, Phys. Lett. **B236** (1990) 144.
M.R. Douglas and S.H. Shenker, Nucl. Phys. **B335** (1990) 635.
D.J. Gross and A.A. Migdal, Phys. Rev. Lett. **64** (1990) 127.
- [2] F. David, Nucl. Phys. **B487** (1997) 633; G. Thorleifsson and B. Petersson, hep-lat/9709072; J. Ambjorn, K.N. Anagnostopoulos and G. Thorleifsson, hep-lat/9709025.
- [3] L. Alvarez-Gaume, J.L.F. Barbon and C. Crnkovic, Nucl. Phys. **B394** (1993) 383.
- [4] A. Mikovic and W. Siegel, Phys. Lett. **B240** (1990) 363; J. Ambjorn and S. Varsted, Phys. Lett. **B257** (1991) 305.
- [5] E. Marinari and G. Parisi, Phys. Lett. **B240** (1990) 375; S. Chaudhuri and J. Polchinski, Phys. Lett. **B339** (1994) 309; A. Jevicki and J.P. Rodrigues, Phys. Lett. **B268** (1991) 53; A. Dabholkar, Nucl. Phys. **B368** (1992) 293.
- [6] T. Banks, W. Fischler, S.H. Shenker and L. Susskind, Phys. Rev. **D55** (1997) 5112.
- [7] E. Witten, Nucl. Phys. **B433** (1995) 85.
- [8] N. Ishibashi, H. Kawai, Y. Kitazawa and A. Tsuchiya, Nucl. Phys. **B498** (1997) 467.
- [9] E. Witten, Nucl. Phys. **B460** (1996) 335.
- [10] M. Fukuma, H. Kawai, Y. Kitazawa and A. Tsuchiya, hep-th/9705128.
- [11] S.R. Das, Rev. Mod. Phys. **59** (1987) 235.
- [12] T. Eguchi and H. Kawai, Phys. Rev. Lett. **48** (1982) 1063.
- [13] G. Bhanot, U. Heller and H. Neuberger, Phys. Lett. **113B** (1982) 47.
- [14] A. Gonzalez-Arroyo and M. Okawa, Phys. Rev. **D27** (1983) 2397.
- [15] J. Nishimura, Mod. Phys. Lett. **A11** (1996) 3049.
- [16] D.J. Gross and E. Witten, Phys. Rev. **D21** (1980) 446.
- [17] M. Creutz, Phys. Rev. **D21** (1980) 2308.

- [18] K. Fabricius and O. Haan, Phys. Lett. **B143** (1984) 459.
- [19] N. Cabibbo and E. Marinari, Phys. Lett. **119B** (1982) 387.
- [20] V.A. Kazakov and I.K. Kostov, Nucl. Phys. **B176** (1980) 199.
- [21] Yu.M. Makeenko and A.A. Migdal, Phys. Lett. **88B** (1979) 135.
- [22] N. Kitsunezaki and J. Nishimura, hep-th/9707162.
- [23] T. Suyama and A. Tsuchiya, hep-th/9711073.